Available online at www.sciencedirect.com

ScienceDirect

Procedia Engineering 199 (2017) 790–795

Procedia Engineering

www.elsevier.com/locate/procedia

X International Conference on Structural Dynamics, EURODYN 2017

Destabilizing damping effect on flat-plate vibrations due to flow-induced flutter

Luca Pigolotti[a,*], Claudio Mannini[a], Gianni Bartoli[a]

[a] *CRIACIV/Department of Civil and Environmental Engineering, University of Florence, Florence 50139, Italy*

Abstract

This paper discusses a case of destabilizing contribution of damping, observed for a flat-plate model vibrating in the cross-flow direction (heaving) and in the rotational degree of freedom (pitching) due to the flow-induced classical-flutter instability. This aeroelastic system can be employed in energy-harvesting applications, where the power extraction corresponds to an equivalent mechanical damping in the heaving motion component. The damping influence was investigated through parametric linear analyses and wind-tunnel tests, discussing the features of both the instability threshold and the system response in the post-critical regime of oscillation. For specific sets of the governing parameters, high-damped configurations get unstable earlier compared to the low-damped case, and show a post-critical motion characterised by a larger pitching amplitude and a pitching-to-heaving phase close to the quadrature.

Peer-review under responsibility of the organizing committee of EURODYN 2017.

Keywords: Classical Flutter; Sub-Critical Bifurcation; Post-Critical Response; Damping; Wind-Tunnel Tests

1. Introduction

The dynamic instability of some mechanical systems can be fostered by increments of damping. This is a well-known phenomenon that can occur in nonconservative mechanical/structural engineering systems, such as Ziegler's discrete column [1] and Beck's or Plüfger's continuous columns (*e.g.* [2,3]) when subjected to a follower axial force. In these cases, theoretical models allowed explaining analytically the damping-induced destabilization (*e.g.* [4–8]). However, very few experimental proofs are available so far (*e.g.* [9,10]).

A similar behaviour can also be encountered in flow-induced-vibration problems, such as for cantilever flexible plates in axial flow [11] and for rigid systems elastically suspended to oscillate with transverse (heaving, η) and rotational (pitching, α) components [12,13]. In the latter case, the aeroelastic instability of classical flutter [14] governs the incipient motion. Nevertheless, so far the effect of damping has been only marginally discussed [12–14].

This work focuses on the heaving-pitching response induced by the classical-flutter excitations on the sectional model of a flat plate (Fig. 1). It originates for energy-harvesting applications of flutter-induced vibrations (*e.g.* [15–17]; see also [18] for a detailed review of the state of the art about energy-harvesting systems). In this framework,

* Corresponding author. Tel.: +39-055-275-8858
E-mail address: luca.pigolotti@dicea.unifi.it

1877-7058
Peer-review under responsibility of the organizing committee of EURODYN 2017.
10.1016/j.proeng.2017.09.076

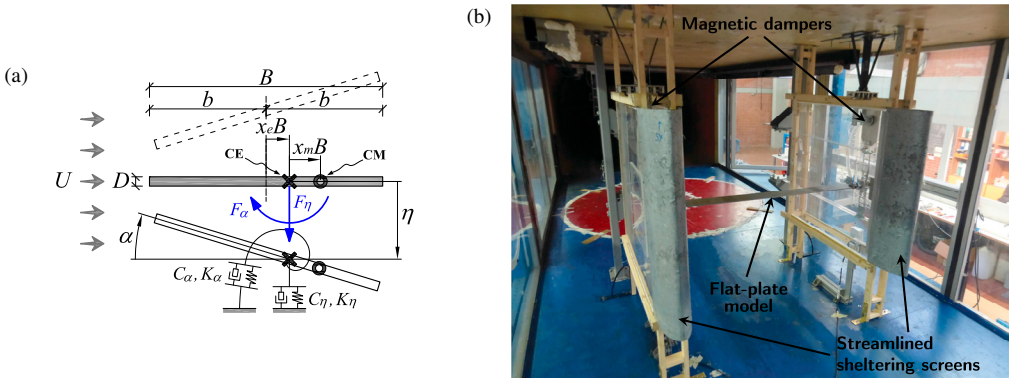

Fig. 1: (a) Schematic of the two-degree-of-freedom flutter problem, describing a cross section of the model in (b) during the motion. (b) View of the aeroelastic setup inside the wind tunnel, with the sheltering screens enforcing a two-dimensional flow.

increments of mechanical damping in the heaving motion component can preliminary simulate the operation of an energy-conversion apparatus [17]. Moreover, post-critical oscillations with large amplitudes are required to obtain effective power generators [17,18]. Thus, the understanding of the system response, at the instability threshold and in the post-critical regime, with respect to the heaving damping is of fundamental importance.

The energy transfer between the airstream and the structure modifies the modal coupling in the fluid-structure system, producing a loss of damping in one mode at the flutter critical condition [14]. Then, a massive flow separation occurs as the motion amplitude increases, inducing nonlinear effects in the aerodynamic loads and contributing to drive the system to limit-cycle oscillations. The ensuing amplitude-velocity path typically manifests very large amplitudes in both the degrees of freedom, which increase with the flow velocity, after a steep initial jump [18–20]. So far, reliable analytical models are available only for the self-excited loads at the incipient motion [14]. Therefore, semi-empirical models and computational simulations [21] or experimental approaches [19,20] are required to predict the large-amplitude response. In the present work, linear analyses were performed to explore parametrically the critical condition (Section 2). Then, a wind-tunnel setup was specifically developed to observe the large-amplitude motion (Section 3.1) and to verify experimentally the damping influence (Section 3.2).

2. Linear analyses

The two-dimensional flutter problem is illustrated in Fig. 1a, where the two-degree-of-freedom (2-DoF) motion is described through the displacement variables $\eta(t) = \hat{\eta}e^{i\omega t}$ and $\alpha(t) = \hat{\alpha}e^{i(\omega t+\hat{\phi})}$. Thereafter, the following dimensionless state-space variables can be defined: $\ddot{\overline{\eta}} = \ddot{\eta}/B\omega^2$, $\dot{\overline{\eta}} = \dot{\eta}/B\omega$, $\overline{\eta} = \eta/B$ and $\ddot{\overline{\alpha}} = \ddot{\alpha}/\omega^2$, $\dot{\overline{\alpha}} = \dot{\alpha}/\omega$, $\overline{\alpha} = \alpha$, where $\omega = 2\pi n$ is the flutter circular frequency. Then, assuming small harmonic displacements, the linear analytical model of Theodorsen [14] was applied to describe the dimensionless flow-induced loads $\overline{F_\eta} = F_\eta/qlB$ and $\overline{F_\alpha} = F_\alpha/qlB^2$, where $q = \frac{1}{2}\rho U^2$ the flow kinetic pressure (being ρ and U the flow density and speed), and l is the model span. Therefore, the instability threshold is governed by the following equation:

$$\begin{cases} \mu\left[\ddot{\overline{\eta}} + 2\xi_{\eta 0}\dfrac{\sqrt{X}}{\gamma_n}\dot{\overline{\eta}} + \dfrac{X}{\gamma_n^2}\overline{\eta} + x_m\ddot{\overline{\alpha}}\right] = \dfrac{\overline{F_\eta}}{K^2} = -\dfrac{\pi}{2}\left[\ddot{\overline{\eta}} + \dfrac{\dot{\overline{\alpha}}}{K} - x_e\ddot{\overline{\alpha}}\right] - C'_{F_\eta}C(k)\left[\dfrac{\dot{\overline{\eta}}}{K} + \dfrac{\overline{\alpha}}{K^2} + \left(\dfrac{1}{4} - x_e\right)\dfrac{\dot{\overline{\alpha}}}{K}\right] \\ \mu r_\alpha^2\left[\ddot{\overline{\alpha}} + 2\xi_{\alpha 0}\sqrt{X}\,\dot{\overline{\alpha}} + X\,\overline{\alpha} + \dfrac{x_m}{r_\alpha^2}\ddot{\overline{\eta}}\right] = \dfrac{\overline{F_\alpha}}{K^2} = \dfrac{\pi}{2}\left[x_e\ddot{\overline{\eta}} - \left(\dfrac{1}{4} - x_e\right)\dfrac{\dot{\overline{\alpha}}}{K} - \left(\dfrac{1}{32} + x_e^2\right)\ddot{\overline{\alpha}}\right] + \\ \qquad\qquad + C'_{F_\alpha}C(k)\left[\dfrac{\dot{\overline{\eta}}}{K} + \dfrac{\overline{\alpha}}{K^2} + \left(\dfrac{1}{4} - x_e\right)\dfrac{\dot{\overline{\alpha}}}{K}\right] \end{cases} . \quad (1)$$

In Eq. (1), $\sqrt{X} = n_{\alpha 0}/n$ is a nondimensional form of the flutter frequency n, being $n_{\alpha 0}$ the pitching frequency of oscillation in still air. Moreover, $K = \omega B/U = 2\pi/U_R$ is the reduced frequency of oscillation, being U_R the reduced flow speed. C'_{F_η} and C'_{F_α} are the slopes of lift and moment aerodynamic coefficients, which for a flat plate are equal

Table 1: Dynamic parameters of a selected subset of the tested configurations.

Code	ρ [kg/m^3]	I_η [kg]	I_α [kg m^2]	S [kg m]	$n_{\eta 0}$ [Hz]	$n_{\alpha 0}$ [Hz]	$\xi_{\eta 0}$ [%]	$\xi_{\alpha 0}$ [%]	x_e [−]	μ [−]	x_m [−]	r_α [−]	γ_n [−]
L13	1.20	8.49	0.014	0.046	1.83	2.27	0.05	1.04	−0.25	1399	0.05	0.40	1.24
L14	1.22	"	"	"	"	"	9.38	"	"	1377	"	"	"
L15	1.21	"	"	"	"	"	14.57	"	"	1388	"	"	"
L16	1.23	8.53	0.018	0.048	1.98	2.00	0.05	0.88	"	1375	0.06	0.45	1.01
L17	1.22	"	"	"	"	"	8.99	"	"	1387	"	"	"
L18	"	"	"	"	"	"	14.98	"	"	1392	"	"	"

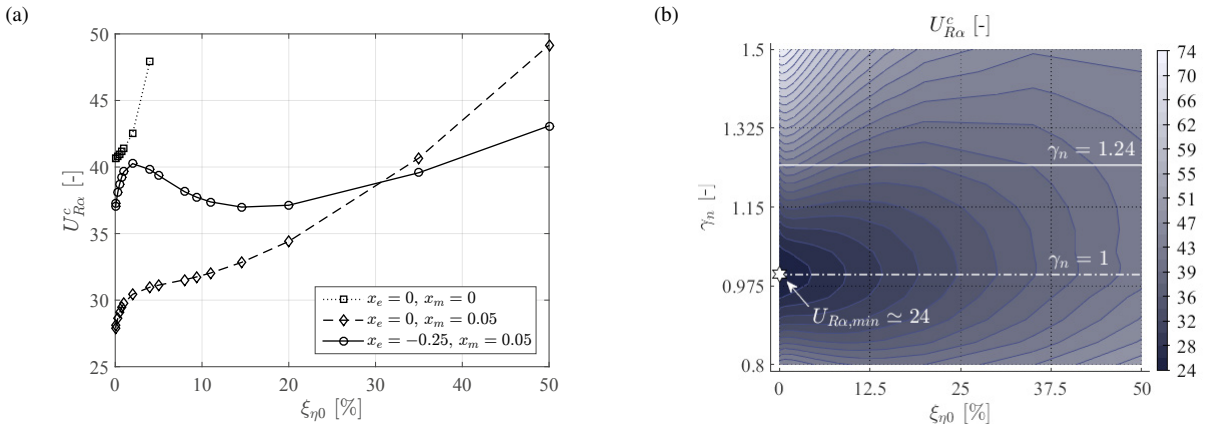

Fig. 2: (a) Nondimensional flutter critical flow speed against heaving damping for different positions of the mass centre and elastic axis; (b) evolution of $U^c_{R\alpha}$ in the $\xi_{\eta 0} - \gamma_n$ space. In both cases, the other dynamic parameters are those of configuration L13.

respectively to 2π and $2\pi(1/4 + x_e)$. $C(k)$ is Theodorsen's circulatory function depending on $k = \omega b/U = K/2$. Clearly, Theodorsen's model is linear with respect to the motion components and their derivatives. The heaving and pitching damping ratios, respectively $\xi_{\eta 0}$ and $\xi_{\alpha 0}$, refer to the internal damping forces. External damping forces are contained in $\overline{F_\eta}$ and $\overline{F_\alpha}$ and vary with the flow speed. Both internal and external contributions are linear viscous terms. The other dimensionless parameters that play a role in the linearised flutter problem are: the elastic-axis eccentricity $x_e = e/B$ (positive if downstream of the section midchord); the mass-centre eccentricity $x_m = a/B = S/I_\eta B$ (positive if downstream of the elastic centre), where S is the static mass unbalance and I_η the heaving inertia; the mass-ratio $\mu = 2I_\eta/\rho B^2 l$; the polar-inertia radius $r_\alpha = B\sqrt{I_\alpha/I_\eta}$, where I_α is the pitching inertia; the frequency ratio $\gamma_n = n_{\alpha 0}/n_{\eta 0}$, where $n_{\eta 0}$ and $n_{\alpha 0}$ are the heaving and pitching oscillation frequencies. The mechanical frequencies and damping ratios refer to the corresponding uncoupled system ($S = 0$) in still air.

The linear analyses were performed to explore the influence of the dynamic parameters of the system on the instability threshold. They were arranged on the basis of the configurations tested in the wind tunnel, referring to the dynamic parameters reported in Table 1. In this type of dynamic problem, the stability parameter is the flow speed U. The critical value U^c can be expressed in dimensionless form as $U^c_R = U^c/nB$ or $U^c_{R\alpha} = U^c/n_{\alpha 0}B$, and the second option has been chosen here.

The system stability is very sensitive to the positions of the elastic centre x_e and of the mass centre x_m, as well as to the frequency ratio γ_n. Fig. 2a shows the predictions of $U^c_{R\alpha}$ for different combinations of elastic- and mass-centre positions, as a function of the heaving damping. It is apparent that a small mass unbalance of $x_m = 0.05$ is able to reduce significantly the critical flow speed compared to the symmetric configuration (*i.e.* with $x_e = 0$, $x_m = 0$). Nevertheless, for the given set of the other dynamic parameters ($\xi_{\alpha 0} = 1.04\%$, $\mu = 1399$, $r_\alpha = 0.4$, $\gamma_n = 1.24$), the destabilizing effect of damping occurs only in the case of configurations with an eccentricity of the elastic centre ($x_e = -0.25$, $x_m = 0.05$). This combination represents the specific case of systems derived from configuration L13, for which the minimum value of the critical speed occurs for a heaving-damping value around 15%. It is worth highlighting that the presence of the mass unbalance is required to observe the instability for high-damped

configurations [20], thus also to encounter a dissipation-induced destabilization (as discussed in the case of Plüfger's column in [2]). The reasons standing behind the choice of the values of x_m and x_e can be found in [18].

Moreover, Fig. 2b displays the critical-flow-speed evaluation in the $\xi_{\eta 0} - \gamma_n$ space, for configurations derived from L13 (Table 1). It is clear that the occurrence of the destabilizing effect of damping depends of the still-air frequency ratio. The systems with frequency ratio close to unity are the most unstable. They show a minimum value of the critical flow speed for $\xi_{\eta 0} = 0$, which then increases by augmenting the damping. By contrast, low-damped systems with γ_n far from unity (larger or smaller) get unstable at values of $U_{R\alpha}$ much higher than for $\gamma_n = 1$, but the critical flow speed tends to approach a value close to the one corresponding to $\gamma_n = 1$ as the heaving damping increases. This behaviour explains the destabilizing effect of damping for the configurations derived from L13, the latter represented in Fig. 2b by the horizontal line corresponding to $\gamma_n = 1.24$. In addition, the gradients in the $U_{R\alpha}$ map indicate that the damping effect is more pronounced for systems with frequency ratio larger than unity.

The other dynamic parameters, and above all the pitching damping ξ_α, can also affect the system stability. In particular, the destabilizing effect of damping may depend on the ratio of heaving to pitching damping, rather than on their individual values, as pointed out in [3] for Ziegler's column.

3. Wind-tunnel tests

3.1. Aeroelastic setup

Experiments were conducted in the open-circuit wind tunnel of CRIACIV in Prato, Italy. A specific aeroelastic setup (Fig. 1b) was designed to enable a large-amplitude motion with vertical (or heaving, η) and rotational (or pitching, α) components. The heaving elastic suspension was provided by a system of coil and leaf springs, while clock springs were used for the pitching suspension. The damping of the heaving motion was controlled through eddy-current-based magnetic dampers, simulating the energy extraction. The damping ratio $\xi_{\eta 0}$ was increased up to values of about 15% in the present tests. The steel model (Fig. 1b) was 100 mm wide (B), 4 mm deep (D) and 1008 mm long (l), the smaller dimension D facing the wind. The model ends were connected to the elastic suspension through a device, which allowed controlling the eccentricity of the elastic centre. It was also possible to add known masses so to shift the mass-centre eccentricity. Reynolds number was in the range 33,000 to 120,000 ($Re = UB/\nu$, with ν=0.15 cm^2/s). The mean flow speed U was measured by a Prandtl probe, installed upstream of the model, and then corrected through known flow maps to infer the velocity at the model centreline. The heaving motion component was recorded through analog laser displacement transducers, while two accelerometers were installed for the pitching component. The frequency sampling was 2000 Hz. The maximum blockage ratio was about 6.25%, reached for rotations of 90°. Screens having a NACA-0020 nose were used to shelter the suspension system from the oncoming flow, avoiding unwanted aeroelastic effects and ensuring two-dimensional flow. The present tests were conducted in smooth flow conditions, with a free-stream turbulence intensity of about 0.7%.

3.2. Experimental results

The motion of the system is described in terms of the amplitude-velocity patterns of the heaving and pitching components during the limit-cycle oscillations. Moreover, the vibration frequency and the pitching-to-heaving phase shift are evaluated. The system response was observed for both increasing and decreasing flow speed. This emphasized the sub-critical bifurcation, which was always found to characterise the flutter instability.

Fig. 3 shows the response of the systems derived from configuration L16, having a still-air frequency ratio close to unity, and from configuration L13, for which the still-air frequency ratio is about 1.24. As predicted by the linear analyses, an increment of the heaving damping has a stabilizing effect in the case of $\gamma_n \simeq 1$. The instability onset is postponed, and the amplitude of the motion is reduced, especially the heaving component. By contrast, the post-critical response of the system with a frequency ratio significantly larger than unity is very different when the heaving damping is increased. Alternatively, not only the critical flow speed of the high-damping configurations is markedly reduced, but also the amplitude of the pitching motion is significantly enhanced, while the heaving component maintains roughly the same magnitude. Thus, the destabilizing effect of damping is also confirmed in terms of post-critical response.

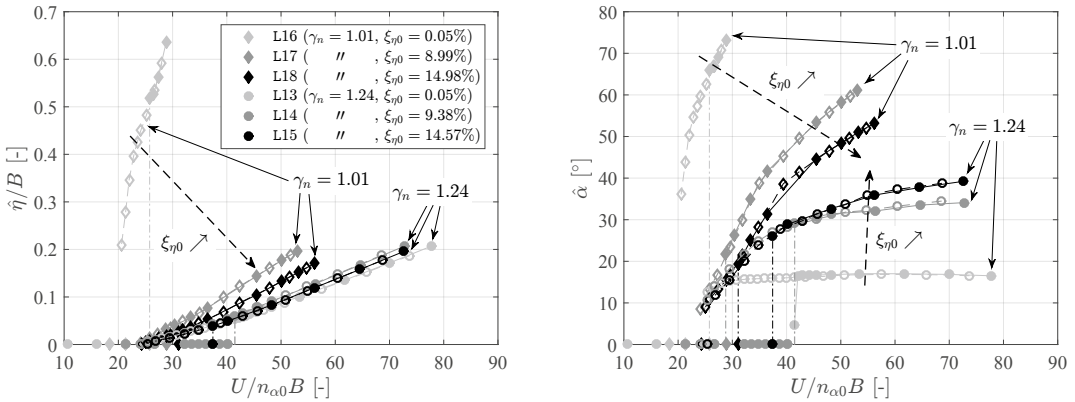

Fig. 3: Amplitude-velocity curves of heaving (left) and pitching (right) displacements during the large-amplitude steady-state motion, for different values of the still-air frequency ratio γ_n and heaving damping $\xi_{\eta 0}$.

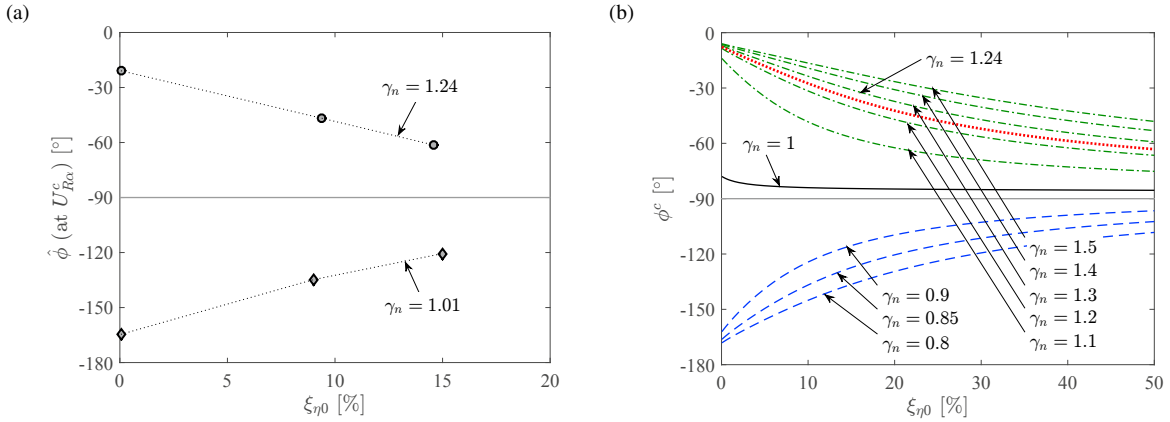

Fig. 4: Pitching-to-heaving phase shift evaluated in the experiments for the steady-state oscillations at the critical flow speed (a), and calculated through the linear analysis (b).

Increments of heaving damping are also responsible for modifying the response toward a quadrature-phase motion, as it is clear observing Fig. 4a. This behaviour was also predicted by the linear analyses (Fig. 4b), although the values of the pitching-to-heaving phase are different from those obtained experimentally. In fact, the linear analysis provides information on the incipient motion, while the phase evaluated in the experiments refers to the steady-state large-amplitude oscillations at the critical flow speed. The excitation mechanisms that govern the two regimes are different, but the results are qualitatively in good agreement.

Furthermore, the system response seems to approach a limit behaviour for very high levels of $\xi_{\eta 0}$, as pointed out by the trends of the motion amplitude (Fig. 3) and phase shift (Fig. 4a). This is also suggested by the linear analysis, since the phase of the motion calculated for different values of the still-air frequency ratio tends to get close to $-90°$ as $\xi_{\eta 0}$ increases (Fig. 4b).

4. Conclusions

The flutter-induced response of a rigid flat plate, elastically suspended so to oscillate in heaving and pitching, was evaluated focusing on the role of the heaving damping. A parametric investigation of the features of the instability threshold was carried out through linear analyses. Then, wind-tunnel experiments were conducted through a specific

aeroelastic setup allowing for large-amplitude motion, in which eddy-current dampers were used to control the heaving damping.

It is found that a small mass unbalance is necessary for the system to get unstable when subjected to high levels of heaving damping, since it enables a faster energy exchange between the motion components. Then, a destabilizing effect produced by the heaving damping is observed when the still-air frequency ratio is significantly removed from unity and the elastic centre is located at the upstream quarter-chord point. In this case, the system is able to oscillate even for high levels of heaving damping by adjusting its response so to find a different dynamic equilibrium, which was characterised by larger pitching amplitudes and nearly unchanged heaving amplitudes. The pitching-to-heaving phase lag also varied, approaching -90° when the heaving damping is increased. Finally, it can be observed that the damping-induced destabilization is a consequence of the saturation of the system response, which approaches the one of the configuration with unitary still-air frequency ratio for very high levels of heaving damping.

Acknowledgements

The authors wish to thank Dr. Tommaso Massai and Dr. Antonino Maria Marra for the support during the tests.

References

[1] H. Ziegler, Die Stabilitätskriterien der Elastomechanik, Archive of Applied Mechanics 20 (1952) 49–56.
[2] M. Tommasini, O. N. Kirillov, D. Misseroni, D. Bigoni, The destabilizing effect of external damping: singular flutter boundary for the Pflüger column with vanishing external dissipation, Journal of the Mechanics and Physics of Solids 91 (2016) 204–215.
[3] A. Luongo, F. D'Annibale, M. Ferretti, Hard loss of stability of Ziegler's column with nonlinear damping, Meccanica 51 (2016) 2647–2663.
[4] G. Herrmann, C. Jong, On the destabilizing effect of damping in nonconservative elastic systems, Journal of Applied Mechanics 32 (1965) 592–597.
[5] V. V. Bolotin, N. I. Zhinzher, Effects of damping on stability of elastic systems subjected to nonconservative forces, International Journal of Solids and Structures 5 (1969) 965–989.
[6] M. A. Langthjem, Y. Sugiyama, Dynamic stability of columns subjected to follower loads: a survey, Journal of Sound and Vibration 238 (2000) 809–851.
[7] O. N. Kirillov, F. Verhulst, Paradoxes of dissipation-induced destabilization or who opened Whitney's umbrella?, ZAMM-Journal of Applied Mathematics and Mechanics/Zeitschrift für Angewandte Mathematik und Mechanik 90 (2010) 462–488.
[8] A. Luongo, F. D'Annibale, On the destabilizing effect of damping on discrete and continuous circulatory systems, Journal of Sound and Vibration 333 (2014) 6723–6741.
[9] D. Bigoni, G. Noselli, Experimental evidence of flutter and divergence instabilities induced by dry friction, Journal of the Mechanics and Physics of Solids 59 (2011) 2208–2226.
[10] S. Saw, W. Wood, The stability of a damped elastic system with a follower force, Journal of Mechanical Engineering Science 17 (1975) 163–179.
[11] S. Michelin, O. Doaré, Energy harvesting efficiency of piezoelectric flags in axial flows, Journal of Fluid Mechanics 714 (2013) 489–504.
[12] R. A. Frazer, W. J. Duncan, A. R. Collar, Elementary Matrices and some Applications to Dynamics and Differential Equations, Cambridge University Press, 1938.
[13] R. A. Frazer, On the power input required to maintain forced oscillations of an aeroplane wing in flight, Technical Report 1872, Aeronaut. Research Com., R. & M., 1939.
[14] Y.-C. Fung, An introduction to the theory of aeroelasticity, Dover Publications, Inc., New York (US), 2008.
[15] K. Isogai, M. Yamasaki, M. Matsubara, T. Asaoka, Design study of elastically supported flapping wing power generator, in: International Forum on Aeroelasticity and Structural Dynamics, Amsterdam, 2003.
[16] M. Bryant, E. Garcia, Modeling and testing of a novel aeroelastic flutter energy harvester, Journal of Vibration and Acoustics 133 (2011) 011010.
[17] L. Pigolotti, C. Mannini, G. Bartoli, K. Thiele, Critical and post-critical behaviour of two-degree-of-freedom flutter-based generators, Journal of Sound and Vibration (accepted).
[18] L. Pigolotti, On the flutter response of two-degree-of-freedom flat plates for energy harvesting applications, Ph.D. thesis, Dept. of Civil and Environmental Engineering, University of Florence, Italy, and Dept. of Architecture, Civil Engineering and Environmental Sciences, University of Braunschweig - Institute of Technology, Germany, 2016.
[19] X. Amandolèse, S. Michelin, M. Choquel, Low speed flutter and limit cycle oscillations of a two-degree-of-freedom flat plate in a wind tunnel, Journal of Fluids and Structures 43 (2013) 244–255.
[20] L. Pigolotti, C. Mannini, G. Bartoli, Destabilizing effect of damping on the post-critical oscillations of flat plates, Meccanica (2017) DOI: 10.1007/s11012-016-0604-y.
[21] B. Lee, S. Price, Y. Wong, Nonlinear aeroelastic analysis of airfoils: bifurcation and chaos, Progress in Aerospace Sciences 35 (1999) 205–334.